

Field Measurement And Simulation of 132 kV Oil-Filled Submarine Cables

Bjørn Gustavsen, Hans Kristian Høidalen, and Trond M. Ohnstad

Abstract—High-voltage cables with paper-oil based insulation are still widely used in electric power systems. One issue with EMTP-type modeling and simulation of such cables is that the permittivity of the insulation is frequency-dependent, thereby contributing to the dispersion of traveling waves. This frequency dependency is not taken into account in currently available EMTP-type programs. This paper presents field measurements from step voltage excitations on three different oil-filled cables with steel armoring. The waveforms are compared to EMTP-type simulations, demonstrating significant deviations from the measured waveforms. The frequency-dependency of the permittivity is next taken into account using a formula obtained by Breien and Johansen, and the modeling and simulation procedure is repeated. Inclusion of the frequency-dependency is shown to bring the simulation results much closer to the measured waveforms.

Keywords: Electromagnetic transients, armored cable, oil-filled cable, EMTP, simulation, field measurement.

I. INTRODUCTION

UNDERGROUND cables are in EMTP-type simulation programs [1] modeled as a set of tubular conductive shells that are separated by lossless insulation. The per-unit-length (p.u.l.) series impedance is calculated via analytical formulae which consider the frequency-dependent skin effects in conductors and earth [2]. The shunt admittance is calculated analytically by considering the insulation material as lossless with a given relative permittivity. The p.u.l. parameters are used as input for generating parameters for frequency-dependent traveling wave models in the time domain, e.g. FDQ [3] or the Universal Line Model (ULM) [4].

In reality, also the insulation material can exhibit frequency dependent behavior due to relaxation mechanisms. While the permittivity of XLPE insulation remains frequency

independent up to very high frequencies, the permittivity of paper-oil insulation is significantly frequency-dependent at frequencies considered in lightning and switching overvoltages, i.e. below 1 MHz. This frequency-dependency was quantified in [5] and demonstrated to significantly contribute to the attenuation and dispersion of short pulses on long cables. The reason for the dispersion is that the propagation speed of the coaxial wave becomes more frequency-dependent.

In this paper we seek to clarify whether the frequency-dependency of [5] is applicable to other cables, for use in overvoltages studies. For that purpose we have performed measurement of sending end step voltage current responses on three different oil-filled cables installed in a regional 132 kV system. The cables have similar design but different cross-sectional area (95 mm², 120 mm², 400 mm²) and length (1800 m, 2168 m). The measurements are compared to time-domain simulations. Since available EMTP-tool do not allow to enter a frequency-dependent permittivity, we coded the whole procedure in Matlab, from impedance and admittance computations to parameter conversion for ULM, and time domain simulation. Using the Matlab-based tool, we perform a direct comparison of the cable sending end current and assess the effect of taking the permittivity frequency dependency into account.

II. SERIES IMPEDANCE CALCULATIONS

The cable has one core (phase conductor), one metallic screen (lead) and two steel armor layers (inner steel tape and outer wire armor). The following outlines the procedure by Wedepohl for calculating the (4×4) impedance matrix of four coaxially arranged conductors (shells), see Fig. 1.

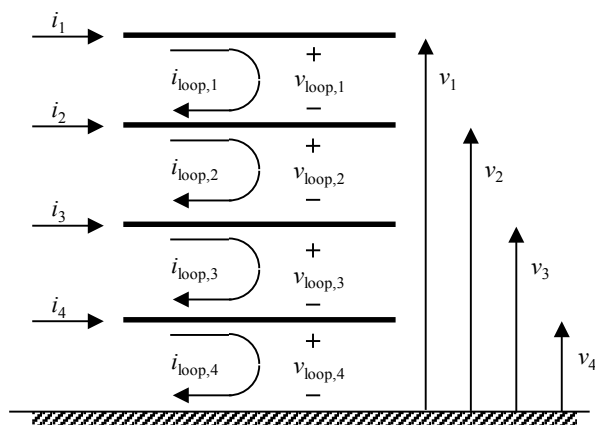


Fig. 1. Loop quantities and phase quantities along a short distance dx .

B. Gustavsen is with SINTEF Energy Research, Trondheim, Norway, (e-mail: bjorn.gustavsen@sintef.no). H. K. Høidalen is with the Department of Electric Power Engineering, Norwegian University of Science and Technology (NTNU), Trondheim, Norway (e-mail: hans.hoidalen@elkraft.ntnu.no), Trond Ohnstad is with Statnett, Oslo, Norway (email: trond.ohnstad@statnett.no).

This work was supported by the Norwegian Research Council (RENERGI Programme) with additional support from DONG Energy, EdF, EirGrid, Hafslund Nett, National Grid, Nexans Norway, RTE, Siemens Wind Power, Statnett, Statkraft, and Vestas Wind Systems.

The voltage drop in terms of loop quantities is

$$-\frac{d\mathbf{v}_{loop}(s)}{dz} = \mathbf{Z}_{loop}(s)\mathbf{i}_{loop}(s) \quad (1)$$

where

$$\mathbf{Z}_{loop} = \begin{bmatrix} Z_a & -Z_2^t & 0 & 0 \\ -Z_2^t & Z_b & -Z_3^t & 0 \\ 0 & -Z_3^t & Z_c & -Z_4^t \\ 0 & 0 & -Z_4^t & Z_d \end{bmatrix} \quad (2)$$

with

$$Z_a = Z_1^{out} + Z_{12}^{ext} + Z_2^{in} \quad (3a)$$

$$Z_b = Z_2^{out} + Z_{23}^{ext} + Z_3^{in} \quad (3b)$$

$$Z_c = Z_3^{out} + Z_{34}^{ext} + Z_4^{in} \quad (3c)$$

$$Z_d = Z_4^{out} + Z_{4g}^{ext} + Z_g \quad (3d)$$

In (3), Z_i^{out} , Z_i^{in} , and Z_i^t denotes respectively the outer and inner surface impedances of the i th shell, and the transfer impedance. Z_{ij}^{ext} is the external impedance associated with the space between the i th and j th shell, with $j=i+1$. The computation of these partial impedances is given in [2].

The relation between loop quantities and phase quantities is given by (4) and (5) with \mathbf{T} given by (6).

$$\mathbf{v}_{loop} = \mathbf{T}^T \mathbf{v} \quad (4)$$

$$\mathbf{i} = \mathbf{T}\mathbf{i}_{loop} \quad (5)$$

$$\mathbf{T} = \begin{bmatrix} 1 & 0 & 0 & 0 \\ -1 & 1 & 0 & 0 \\ 0 & -1 & 1 & 0 \\ 0 & 0 & -1 & 1 \end{bmatrix} \quad (6)$$

Combining (4) and (5) with (1) gives for the impedance in phase quantities

$$-\frac{d\mathbf{v}}{dz} = \mathbf{Z}\mathbf{i} \quad (7)$$

with

$$\mathbf{Z} = \mathbf{T}^{-T} \mathbf{Z}_{loop} \mathbf{T}^{-1} \quad (8)$$

Since we in the field measurement are considering high frequencies only, we do not need to consider the mutual coupling between the cables as the screen and armoring prevents magnetic flux to penetrate the sea.

III. SHUNT CAPACITANCE CALCULATIONS

The capacitance in terms of loop quantities

$$-\frac{di_{loop}(s)}{dz} = \mathbf{Y}_{loop}(s)\mathbf{v}_{loop}(s) \quad (9)$$

where \mathbf{Y}_{loop} is diagonal with entries

$$\mathbf{Y}_{loop} = \text{diag}([Y_a \ Y_b \ Y_c \ Y_d]) \quad (10)$$

The i th entry in (10) is the shunt admittance between shells i and $i+1$. Combining (4) and (5) with (9) gives for the admittance in phase quantities

$$-\frac{d\mathbf{i}}{dz} = \mathbf{Y}\mathbf{v} \quad (11)$$

with

$$\mathbf{Y} = \mathbf{T}\mathbf{Y}_{loop}\mathbf{T}^T \quad (12)$$

IV. FREQUENCY-DEPENDENT PERMITTIVITY

Breien and Johansen have obtained the frequency dependency of oil-impregnated paper from measurements [5]. This frequency dependency is given as

$$\varepsilon_r(s) = 2.5 + \frac{0.94}{1 + (6 \cdot 10^{-9} s)^{0.315}} \quad (13)$$

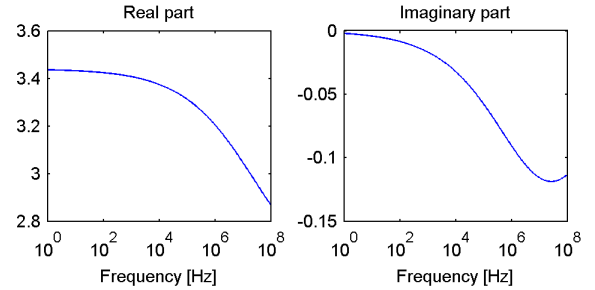


Fig. 2. Permittivity as function of frequency [5].

In our case, the capacitance of the main insulation was measured at 50 Hz, allowing to compute the permittivity at 50 Hz as

$$\varepsilon_{r,50Hz} = \frac{\ln(r_2 / r_1)}{2\pi\varepsilon_0} \quad (14)$$

where r_1 and r_2 are the conductor outer radius and metallic screen inner radius, respectively. The permittivity to be used is then calculated by simple scaling

$$\tilde{\varepsilon}_r(s) = \frac{\varepsilon_{r,50Hz}}{2.5 + 0.94} \left(2.5 + \frac{0.94}{1 + (6 \cdot 10^{-9} s)^{0.315}} \right) \quad (15)$$

and the shunt admittance for (10) becomes

$$Y_a(s) = s \frac{2\pi\varepsilon_0 \tilde{\varepsilon}_r(s)}{\ln \frac{r_2}{r_1}} \quad (16)$$

V. CABLE DATA

Tables I-III describes the data for three cables as used in the modeling. All cable conductors are modeled as a massive conductor with the conductivity adjusted to give the DC resistance stated in the technical data sheet, given the lack of information about the oil-channel in the conductor center. The values used for the armoring conductivity and in particular the permeability are subject to significant uncertainty; however the simulation results are not sensitive to these data as will later be shown in Section VI-B. We have assumed a separation distance of 1 mm between the lead screen and the inner armor, and 2 mm between the inner armor and the outer armor.

TABLE I: 95 mm² cable data used in simulations (20 °C)

Item	R [mm]	t [mm]	σ [S/m]	μ_r
Conductor	9.6		$18.7E6$	1
Insulation		14.5		1
Lead sheath		3.2	$4.6E6$	1
Tape armor		0.5	$5.6E6$	10
Wire armor		5.6	$5.6E6$	10

TABLE II: 120 mm² cable data used in simulations (20 °C)

Item	R [mm]	t [mm]	σ [S/m]	μ_r
Conductor	8.05		$32.11E6$	1
Insulation		12.5		1
Lead sheath		2.2	$4.55E6$	1
Tape armor		0.4	$5.6E6$	10
Wire armor		5.6	$4.4E6$	10

TABLE III: 400 mm² cable data used in simulations (20 °C)

Item	R [mm]	t [mm]	σ [S/m]	μ_r
Conductor	13.15		$39.2E6$	1
Insulation		11.5		1
Lead sheath		2.3	$4.6E6$	1
Tape armor		0.4	$5.6E6$	10
Wire armor		5.0	$4.4E6$	10

In all calculations, the conductivities are recomputed for 5°C by (17) with $\alpha=0.004$ and ρ being the resistivity.

$$\rho = \rho_{@20C} (1 + \alpha(T - 20)) \quad (17)$$

The capacitance of the three cables was measured at 50 Hz, see Table IV. The cable lengths are listed in Table V.

TABLE IV: Measured capacitance

Cable	95 mm ²	120 mm ²	400 mm ²
C [nF/km]	219	217	321

TABLE V: Cable length

Cable	95 mm ²	120 mm ²	400 mm ²
Length [m]	1800	1800	2168

VI. MODEL VALIDATION

A. Validation for 120 mm² Cable Against PSCAD

After calculating the per-unit-length impedance and shunt admittance using the procedure in Section IV, we calculate parameters for the Universal Line Model (ULM) via rational functions and employ it in an EMTP-type simulation in Matlab. In order to validate the Matlab-based tool we have made a direct comparison with a simulation using PSCAD for the 120 mm² cable when ignoring the frequency-dependency of the main insulation. The test conditions are shown in Fig. 3.

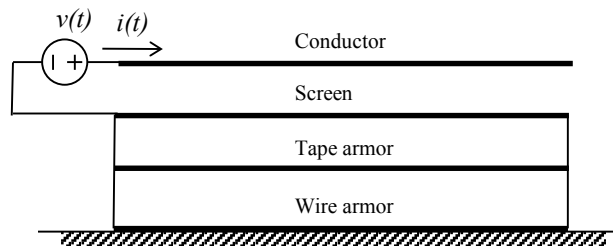


Fig. 3. Unit step voltage application to cable.

Figs. 4 and 5 show the simulated waveforms of the receiving end voltage and sending end currents, respectively. An excellent agreement is achieved, which is not surprising since the Wedepohl formulae are also used by PSCAD.

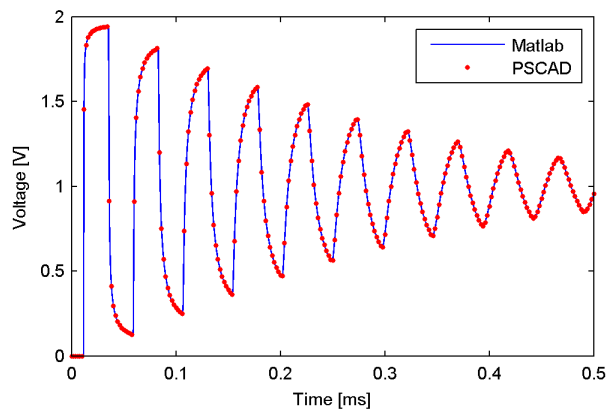


Fig. 4. Matlab vs. PSCAD simulation: Sending end current response

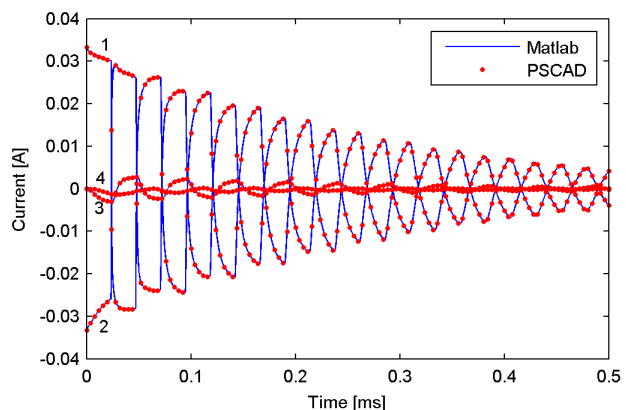


Fig. 5. Matlab vs. PSCAD simulation: Receiving end voltage response. 1: conductor, 2: screen, 3: inner armor, 4: outer armor.

B. Sensitivity Analysis

One major uncertainty is the modeling of the armoring, in particular the permeability to be used. To add to the uncertainty, the armoring may be corroded. Fig. 6 shows that the simulated current wave form of the conductor at the sending end (which is the quantity to be studied) is only weakly sensitive to the assumed armor permeability.

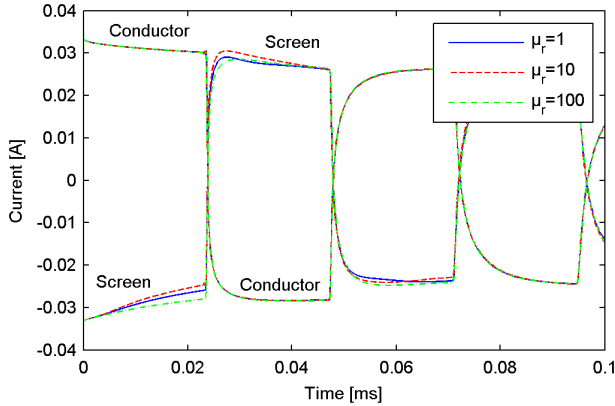


Fig. 6. Sensitivity of sending end conductor current to steel permeability.

VII. COMPARISON WITH FIELD MEASUREMENTS

A. Measurement Setup

A function generator was used for producing a step voltage signal, which was fed into a wide-band amplifier with a low-impedance output. The output signal is fed to the cable end via a coaxial cable as shown in Fig. 7. This setup gives a stiff voltage with a steep wave front. One of the cable termination houses is shown in Fig. 8.

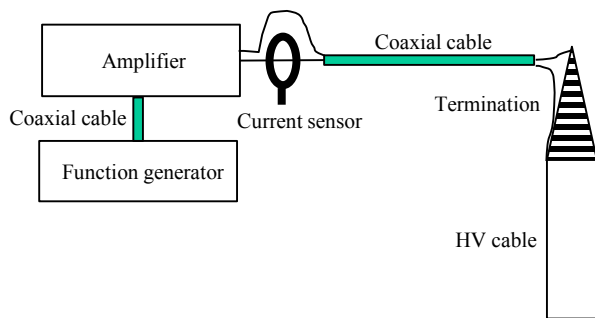


Fig. 7. Connecting the measurement equipment to the cable.



Fig. 8. Cable termination house.

B. 120 mm² Cable

Fig. 9 shows the measurement of applied voltage wave form on the sending end of the 120 mm² cable. This voltage is used in a time domain simulation as an ideal voltage source and applied to the cable model. Fig. 9 also shows the simulated voltage wave form on the cable receiving end, when the permittivity frequency dependency is either ignored or taken into account. This frequency dependency is seen to have a quite noticeable effect on the waveform.

Fig. 10 compares the measured sending end current with that by the simulation. Taking the insulation frequency dependency into account gives much smoother waveforms. This is better seen in the expanded view in Fig 11 where the measurement has been shifted 4 μ s in time to eliminate the phase shift. Clearly, the shape of simulated current agrees much closer with that of the measured current when taking the permittivity frequency dependency into account. The original saw tooth-like wave shape becomes smoother as the wave front is smeared out due to dispersion.

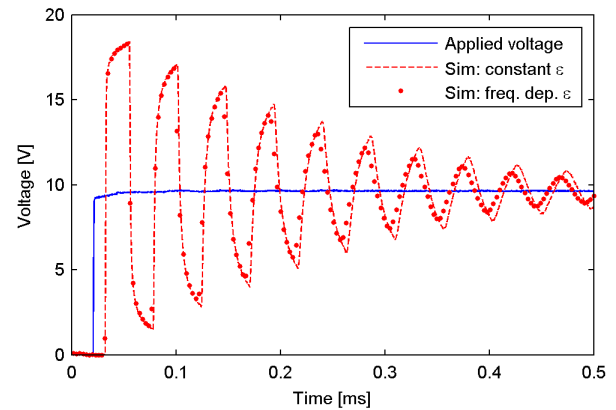


Fig. 9. Applied (measured) voltage and simulation of receiving end voltages.

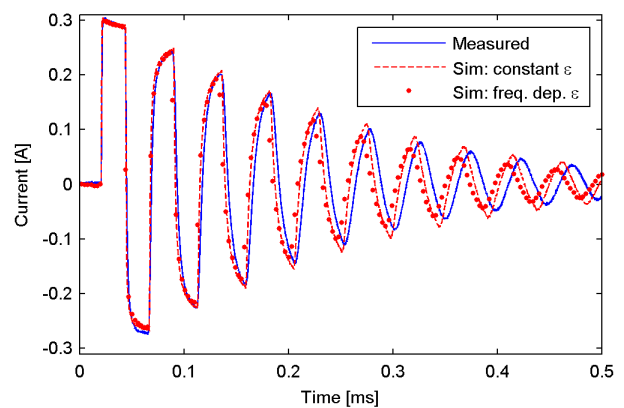


Fig. 10. Sending end conductor current: Measured and simulated.

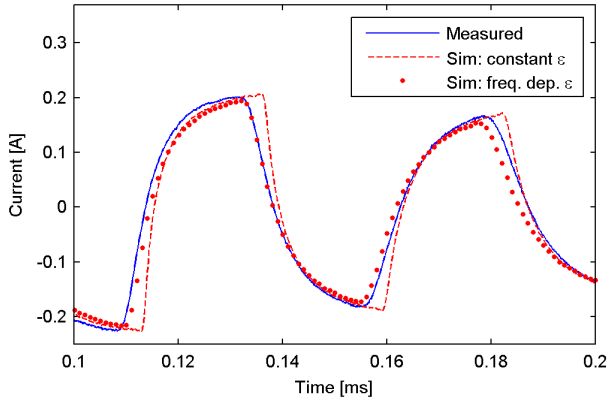


Fig. 11. Sending end conductor current. Close-up. Measurement shifted 4 μ s.

C. 95 mm² Cable

The same procedure was repeated for the 95 mm² cable, see Figs. 12 and 13. As before, the simulated waveform agrees much closer with the measured one when taking the frequency dependency of the permittivity into account.

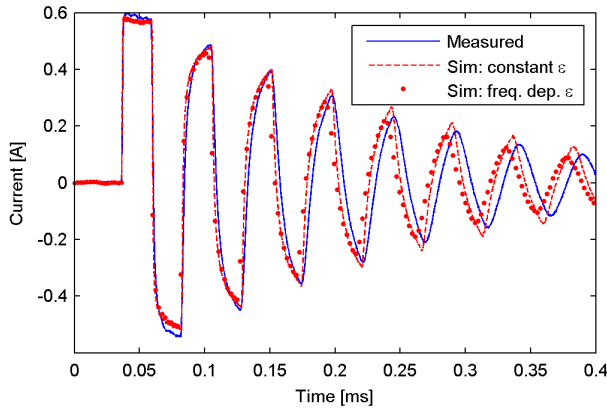


Fig. 12. Sending end conductor current: Measured and simulated.

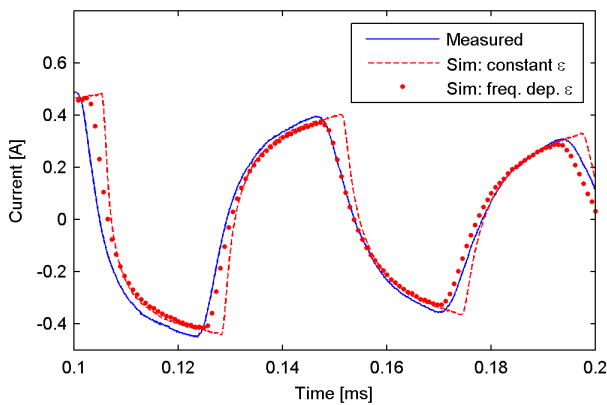


Fig. 13. Sending end conductor current. Close-up. Measurement shifted 4 μ s.

D. 400 mm² Cable

Also for the 400 mm² cable we reach the same conclusion: Taking the permittivity frequency dependency into account gives a more correct wave shape as compared to the measurement, see Figs. 14 and 15.

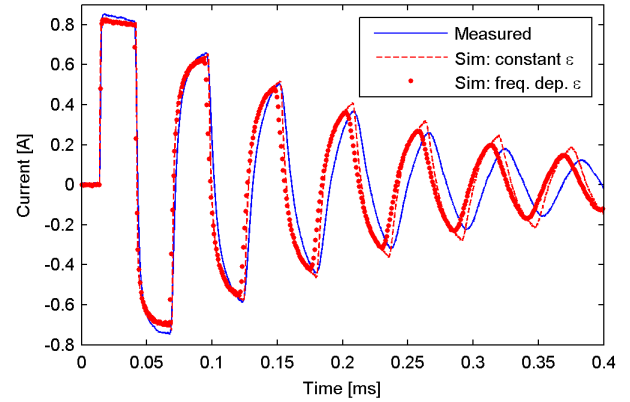


Fig. 14. Sending end conductor current: Measured and simulated.

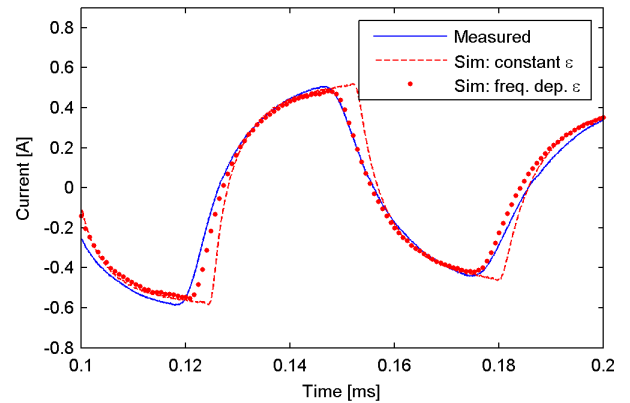


Fig. 15. Sending end conductor current: Close-up. Measurement shifted 5 μ s.

VIII. DISCUSSION

In all simulations, the dominating frequency is slightly higher than in the measurement. This deviation is not surprising since the result is strongly dependent on the distance between the core conductor and the lead sheath. The insulation thickness used in the calculations was that from the cable data sheet. However, the actual thickness may be higher as the one in the data sheet is possibly a guaranteed minimum thickness. Figs. 16 and 17 show the result of increasing the insulation thickness by 1 mm while adjusting permittivity to retain the original capacitance value. The increased inductance is seen to give a nearly perfect agreement with the measurements, for the entire time window.

The good agreement reached in all tests may indicate that the formula by Breien and Johansen is valid for oil-filled cables in general. This is not necessarily true since all cables were of similar design and from the same manufacturer. The same manufacturer also provided test samples for the study by Breien and Johansen. New measurement on cables by a different manufacturer should therefore be carried out to reach more firm conclusions.

All measurements were performed at a very low voltage compared to the actual operating conditions, which may impact the behavior of the steel armoring. However, it was shown in Section VI-B that the simulated sending end current on the phase conductor is not sensitive to the assumed value of the steel permeability.

The reason for the dispersion effect is mainly that the frequency-dependent permittivity makes the propagation velocity more frequency-dependent at high frequencies, see Fig. 18. As a result, the high-frequency components travel faster than the lower frequency components, leading to a deflation of the wavefronts.

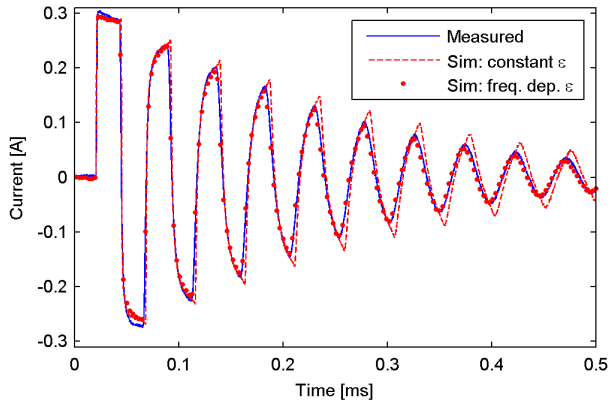


Fig. 16. Sending end conductor current for 120 mm² cable when increasing insulation thickness by 1 mm.

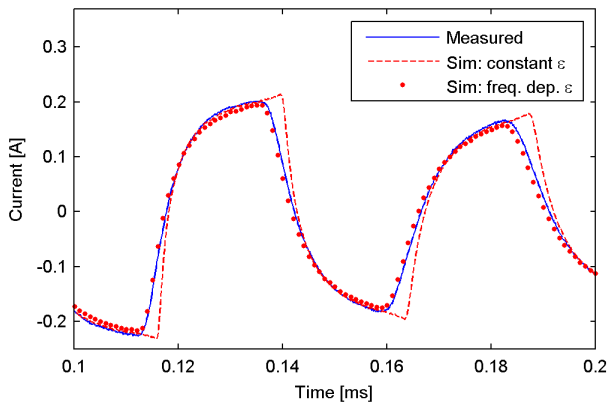


Fig. 17. Sending end conductor current. Close-up of Fig. 16.

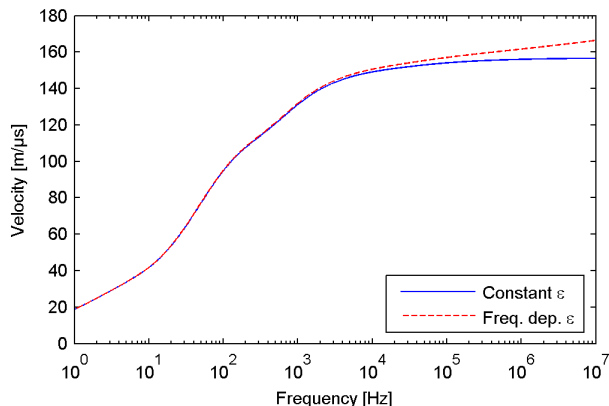


Fig. 18. Propagation velocity.

IX. CONCLUSIONS

This paper compares cable sending end currents against measured waveforms for three different oil-filled cables where one cable end is subjected to a step voltage excitation. It is shown that taking the frequency dependency of the permittivity into account by the Breien-Johansen formula greatly improves the accuracy of the simulation. The formula should be made available in EMTP-type simulation programs as a user-requested feature.

X. ACKNOWLEDGEMENT

The authors thank Oddgeir Rokseth (SINTEF Energy Research) and the staff at Statnett for assistance in the field measurements.

XI. REFERENCES

- [1] H.W. Dommel, ElectroMagnetic Transients Program. Reference Manual (EMTP Theory Book), Bonneville Power Administration, Portland, 1986.
- [2] L.M. Wedepohl and D.J. Wilcox, "Transient analysis of underground power transmission systems; system-model and wave propagation characteristics", *Proc. IEE*, vol. 120, no. 2, pp. 252-259, Feb 1973.
- [3] L. Marti, "Simulation of transients in underground cables with frequency-dependent modal transformation matrices" *IEEE Trans. Power Delivery*, vol. 3, no. 3, pp. 1099-1110, July 1988.
- [4] A. Morched, B. Gustavsen, and M. Tartibi, "A universal model for accurate calculation of electromagnetic transients on overhead lines and underground cables", *IEEE Trans. Power Delivery*, vol. 14, no. 3, pp. 1032-1038, July 1999.
- [5] O. Breien and I. Johansen, "Attenuation of traveling waves in single-phase high-voltage cables", *Proc. IEE*, vol. 118, no. 6, pp. 787-793, June 1971.

XII. BIOGRAPHIES

Bjørn Gustavsen born in Norway in 1965. He received the M.Sc. degree and the Dr.Eng. degree in Electrical Engineering from the Norwegian Institute of Technology (NTH) in Trondheim, Norway, in 1989 and 1993, respectively. Since 1994 he has been working at SINTEF Energy Research where he is currently a Chief Research Scientist. His interests include simulation of electromagnetic transients and modeling of frequency dependent effects in cables and transformers.

Hans Kristian Høidalen Hans Kr. Høidalen (M'05) was born in Norway in 1967. He received his MSc and PhD degrees from the Norwegian University of Science and Technology in 1990 and 1998, respectively. He is now a professor at the same institution with a special interest of power system transients, electrical stress calculations and modeling.

Trond M. Ohnstad was born in Oslo, Norway, on September 15, 1958. He graduated from the Faculty of Electrical Engineering, Oslo College, Oslo, Norway, in 1981. He has completed several special courses on power system planning, insulation coordination, surge protection, power electronics, and HVDC. His employment experience includes the Norwegian State Power Board, the Norwegian State Power Company, and the Norwegian Power Grid Company Statnett. His research interests are insulation coordination and surge protection, power quality, and power system transients.